

Cite this: *Soft Matter*, 2012, **8**, 6409

www.rsc.org/softmatter

HIGHLIGHT

Lipid membranes in contact with aqueous phases of polymer solutions

Rumiana Dimova* and Reinhard Lipowsky

DOI: 10.1039/c2sm25261a

In this highlight, we describe recent developments in research on lipid vesicles encapsulating aqueous two-phase polymer solutions. Special emphasis is given on the morphological changes of the vesicles and the membrane transformations induced by the phase separation process, and on the interactions of the lipid bilayers with the phases. These interactions lead to a variety of interesting wetting phenomena and to the formation of membrane nanotubes. Future directions and possible developments in this research field are also discussed.

Introduction

The interior of living cells is crowded with macromolecules and organelles. The weight fraction of proteins, RNAs and polysaccharides is on the order of 20–30%. Interactions between macromolecules in water can lead to the formation of coexisting aqueous phases. Thus, in the concentrated environment in the cell, local phase separation may occur, involving local composition differences and microcompartmentation, affecting,

e.g., cell functioning and the performance of cytoplasmic proteins.^{1,2}

The phenomenon of phase separation is often observed in solutions of two polymer species. Probably the most well studied aqueous two-phase system (ATPS) based on polymer solutions is the one of poly(ethylene glycol) (PEG) and dextran at polymer concentrations above a few weight percent. This ATPS is widely used in the separation of biomolecules, viruses and cells.³ In this system, each of the two phases is enriched in one of the polymers. In solutions of two oppositely charged polyelectrolytes, a more complex phase behavior can be observed.⁴ For systems with more than two types of neutral polymers, additional phases may

also be formed. Even single-polymer solutions may phase separate under specific temperature or salt conditions.

Aqueous phase separation in the closed environment of lipid vesicles as a model system for biological microcompartments was considered by the group of C. Keating.⁵ The system was employed to study protein redistribution between the phases.^{6–8} In these studies, the phase separation process was induced by temperature changes, while our group⁹ introduced osmotic deflation as a convenient method to induce phase separation in giant vesicles.

Giant lipid vesicles¹⁰ loaded with polymer solutions exhibit several spatial compartments formed by phase

Max Planck Institute of Colloids and Interfaces, Science Park Golm, Potsdam, Germany. E-mail: dimova@mpikg.mpg.de; Fax: +49 (0)331 567 9612; Tel: +49 (0)331 567 9615



Rumiana Dimova

Rumiana Dimova obtained her PhD at Bordeaux University (France) at the end of 1999. Afterwards she joined the Max Planck Institute of Colloids and Interfaces as a postdoctoral fellow, where she became a group leader in 2000. Since then she has led the experimental lab in the Department of Theory and BioSystems. Her main research interests are in the field of membrane biophysics.



Reinhard Lipowsky

Reinhard Lipowsky obtained his PhD in 1982 at the University of Munich. In 1990, he was appointed full professor at the University of Cologne and director at the Forschungszentrum Jülich. Since 1993, he has been a director at the Max Planck Institute of Colloids and Interfaces. He works on fundamental aspects of biomimetic and biological systems.

separation within the vesicle interior.^{6,9,11} Thus, these artificial cell-like systems are a biomimetic setup for studying molecular crowding, fractionation and protein sorting in cells. The polymer weight fractions used in the above-mentioned work were comparable to those in cells.

We employed these cell-sized biomimetic systems to study the wetting behavior of the polymer phases on the membrane,^{9,12} the reorganization of the lipid bilayer arising from molecular crowding¹³ and the resulting morphological shapes adopted by vesicles loaded with ATPS.¹⁴ In the following, we first introduce some basic properties of the PEG–dextran ATPS, and then we review results on the direct effect of this system on the membrane. Finally, we discuss possible further advances and directions in the field.

Aqueous two-phase polymer solutions of dextran and poly(ethylene glycol)

Above a total polymer weight fraction of a few weight percent, aqueous solutions of PEG and dextran demix. The corresponding two-phase region is bounded by the binodal line within the phase diagram of the system; an example is shown in Fig. 1. At concentrations below the binodal the polymer solution is homogeneous. Above the binodal the solution undergoes phase separation and the compositions of the individual phases are given by the tie lines in the phase diagram, see Fig. 1. A variety of methods for tie line determination has been explored in the literature based on the use of different experimental techniques; see *e.g.* ref. 15. Recently, we proposed a relatively simple approach based on density measurements of the phases.¹⁶ The PEG-rich phase is the lighter one. It is characterized by a lower refractive index as compared to the dextran-rich phase, which makes the two phases easily distinguishable when observed in giant vesicles under phase contrast mode, see *e.g.* Fig. 3c.

Because of their simplicity and biocompatibility, ATPSs are widely used in the separation of biomolecules, viruses and cells.³ When biological materials are mixed in an ATPS, they can selectively adsorb at the liquid–liquid interface. The PEG–dextran polymer systems provide

a particularly mild environment for biomolecules and cells because the interfacial tensions found in these systems are extremely low (about 1–100 $\mu\text{N m}^{-1}$).¹⁷ In such polymeric two-phase systems, no detectable denaturation of proteins occurs, in contrast to two-phase systems based on solutions of small molecules, characterized by higher interfacial tensions, typically of the order of tens of mN m^{-1} . Detailed measurements of the interfacial tension as a function of polymer concentration indicate that the critical behavior of the tension is approximately described by mean field theory over the accessible concentration range.¹⁶

Membrane wetting

Liquid droplets at interfaces may exhibit zero or nonzero contact angles corresponding to complete or partial wetting, respectively. As one varies a certain control parameter, such as temperature or liquid composition, the system may undergo a transition from complete to partial wetting. In the following section, we will demonstrate that such a transition can also occur for an aqueous solution in contact with a freely suspended lipid membrane,⁹ and in particular for an aqueous solution enclosed within a vesicle. In the latter case, the substrate is

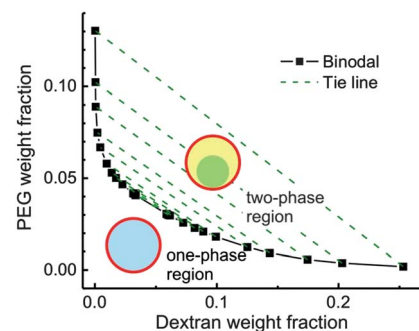


Fig. 1 Binodal and tie lines of the aqueous solution of dextran (molecular weight between 400 and 500 kg mol^{-1}) and PEG (molecular weight 8 kg mol^{-1}) measured at 24 ± 0.5 °C.¹⁶ Below the binodal the polymer solution is homogeneous; above the binodal it undergoes phase separation. The insets schematically illustrate the vesicle membrane (red) enclosing the homogeneous solution (blue) or the two liquid droplets consisting of dextran-rich (green) and PEG-rich (yellow) phases. Adapted with permission from ref. 16. Copyright (2012) American Chemical Society.

the lipid membrane. We then discuss the processes following the wetting transition when the vesicles are deflated. The system of giant vesicles encapsulating two aqueous phases is of particular interest since it enables us to observe the interplay between wetting phenomena and membrane physics. Understanding the behavior of such systems provides insight into processes involving vesicle formation in biological cells. For example, wetting of a membrane by a liquid droplet creates a contact line, which may enhance endocytotic or exocytotic processes. Wetting-induced budding, as discussed below, provides a possible mechanism for the selective vesicle transport in cells as well as for the vesicle shedding¹⁸ involved in membrane traffic and molecule transfer among neighboring cells.

The preparation of GUVs encapsulating ATPSs follows the conventional protocol of electroformation and is described in detail in ref. 9 and 13. The experimental results reviewed here were obtained as follows. The vesicles were formed in polymer solutions in the one phase region at room temperature, *e.g.*, with polymer concentrations 4.05 wt% PEG and 2.22 wt% dextran. Then, they were diluted in an isotonic solution containing 4.41 wt% PEG and 1.45 wt% dextran to make them sediment to the bottom of the observation chamber. To obtain vesicles containing two phases, we raised the polymer concentration above the binodal, see Fig. 1, by stepwise deflation, exposing the vesicles to a hypertonic medium. The compositions of the polymer solutions were selected so that the density of the external medium was lower than that of the dextran-rich phase but higher than that of the PEG-rich phase. This ensures that the vesicles always “stand” on the chamber bottom with the PEG-rich phase pointing upward, see *e.g.* Fig. 2b–f.

Wetting transition

We used giant vesicles encapsulating PEG–dextran solution in the one-phase state, see Fig. 2a. In order to obtain vesicles containing two phases, we raised the polymer concentration above the binodal by deflation, *i.e.*, by exposing the vesicles to a hypertonic medium containing 3.27 wt% sucrose, 3.92 wt% PEG, and 2.14 wt% dextran. Water is forced out of

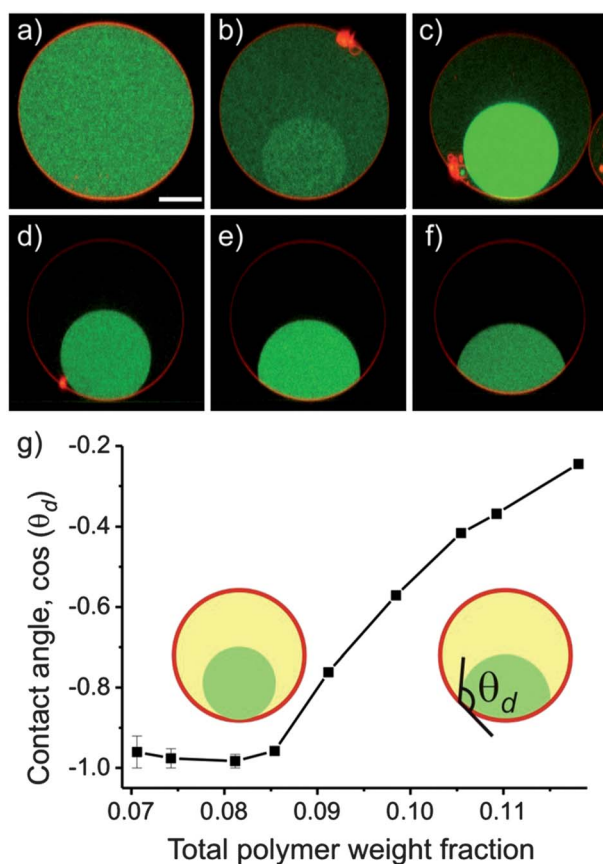


Fig. 2 Phase separation of aqueous polymer solutions enclosed in vesicles at room temperature. The polymer molecular weights are the same as those described in the caption of Fig. 1. The composition of the membrane (red) in mole fractions is 95.9% 1,2-dioleoyl-*sn*-glycero-3-phosphocholine (DOPC), 4.0% galbeta1-3galnacbeta1-4(neuacalpha2-3)galbeta1-4glcbeta1-1'-cer (G_{M1} Ganglioside) and 0.1% 1,2-dipalmitoyl-*sn*-glycero-3-phosphoethanolamine-*N*-(lissamine rhodamine B sulfonyl). (a–f) Confocal micrographs of a vesicle (vertical cross-sections), which contains a dextran-rich drop (green) undergoing a wetting transition as the external osmolarity is increased in a stepwise manner. The encapsulated aqueous solution is initially composed of 4.05 wt% PEG and 2.22 wt% dextran. A small fraction of the dextran (0.52%) is fluorescently labeled with fluorescein isothiocyanate (green). The scale bar corresponds to 20 μm . (g) Cosine of the contact angle θ_d versus total polymer concentration in the vesicle. The weight ratio between dextran and PEG is 0.55. The insets schematically illustrate the dewetted and wetted states, as well as the contact angle. Adapted with permission from ref. 9. Copyright (2008) American Chemical Society.

the vesicle to balance the resulting osmotic pressure and the polymer concentration inside increases, leading to phase separation, see Fig. 2a and b. The part with more intensive green fluorescence in the images presents the dextran-rich phase, and the part with less intensive fluorescence is the PEG-rich phase. The former is heavier than the latter, and thus the dextran-rich droplet is always located at the bottom of the vesicle, see Fig. 2b–f.

When the external osmolarity is further increased, the dextran-rich phase starts to wet the membrane, see Fig. 2d, and the contact area between the dextran-rich phase and the membrane grows with

further vesicle deflation, see Fig. 2d–f. The morphology change of the dextran-rich droplet indicates a wetting transition from complete wetting of the PEG-rich phase or complete dewetting of the dextran-rich phase in Fig. 2c to partial wetting in Fig. 2d–f.

By fitting the vesicle and the drop contours in the acquired images with spherical caps, we obtain the contact angle, θ_d , between the dextran-rich phase and the membrane, see inset in Fig. 2g, under different osmolarity conditions. Because the membrane is permeable only to water but not to the polymers, we can calculate the total polymer concentration

in the vesicle at each deflation step. The cosine of the contact angle θ_d defines the wettability via $\cos(\theta_d) \equiv (\hat{\Sigma}_{pe} - \hat{\Sigma}_{de})/\Sigma_{pd}$. Here $\hat{\Sigma}_{pe}$ and $\hat{\Sigma}_{de}$ are the tensions of the membrane segments in contact with the PEG-rich phase (pe) and the dextran-rich phase (de), respectively, and Σ_{pd} is the tension of the interface between the two polymer phases (pd), see also Fig. 3f. The wettability as a function of the total polymer concentration inside the vesicle is given in Fig. 2g. A sharp change in the contact angle is observed for polymer concentrations around 8.5 wt%, indicating a wetting transition.

The membrane tensions $\hat{\Sigma}_{pe}$ and $\hat{\Sigma}_{de}$ will depend on the molecular structure of the lipid bilayer and on the interactions between the lipid head groups and the two polymer phases. Thus, these tensions can be varied by changing the membrane composition. Of particular interest would be to study wetting phenomena in vesicles containing domains of various compositions. Some work on multicomponent vesicles with domains encapsulating the PEG–dextran ATPS has already been reported in ref. 11 and 19. The tensions $\hat{\Sigma}_{pe}$, $\hat{\Sigma}_{de}$ and Σ_{pd} will also be affected by the mechanical tension within the membrane, which can be manipulated by exerting an external pressure on the vesicle through a micropipette, as we will see in the following section.

Wetting-induced budding

When both phases wet the membrane, the smaller one may bud out of the vesicle body upon further deflation. Fig. 3 shows such an example. The vesicle with two liquid phases is approximately spherical at a low osmolarity ratio between the external medium and the initial internal polymer solution; see Fig. 3c. When the vesicle is further deflated, the dextran-rich phase starts to form a bud away from the PEG-rich phase; see Fig. 3d. The excess area arising from deflation is utilized by the vesicle to undergo morphological changes and a budding transition.¹⁴ In this way, the area of the liquid two-phase interface is decreased significantly. As the osmolarity of the medium is increased further, the dextran-rich phase may form a complete bud¹⁹ leading to a dumbbell-like vesicle where the area of the two-phase interface is almost zero, see the last cartoon in Fig. 3a. The budding direction

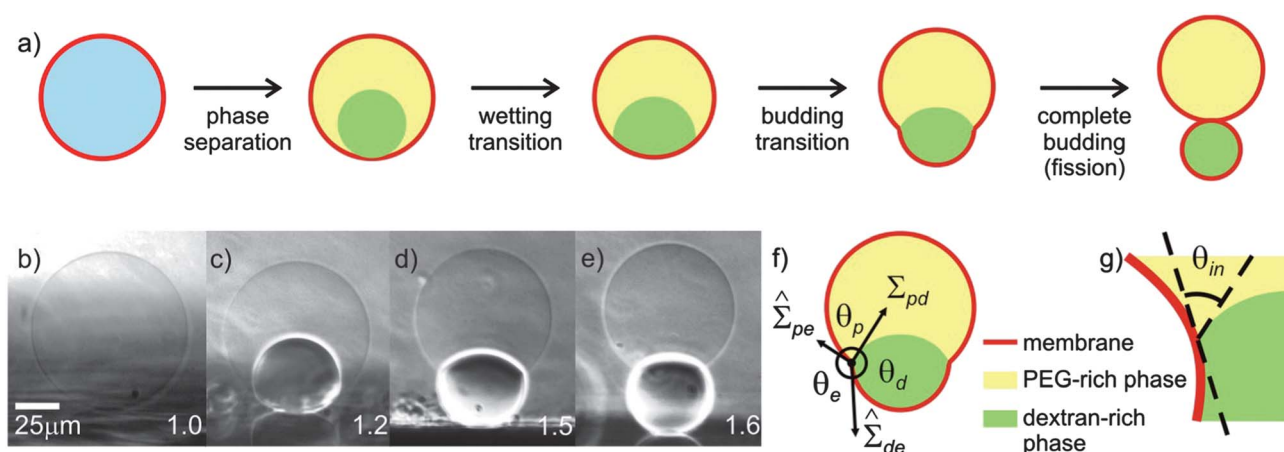


Fig. 3 Response of ATPS-loaded vesicles when exposed to osmotic deflation. (a) Schematic illustration of the steps accompanying the deflation: phase separation within the vesicle, wetting transition, vesicle budding, and fission of the enclosed phases into two membrane-wrapped droplets. (b–e) Side-view phase contrast images of a vesicle sitting on a glass substrate. Adapted with permission from ref. 14. Copyright (2012) American Chemical Society. The vesicle contains the PEG–dextran ATPS. The polymer molecular weights and the membrane composition are the same as in Fig. 2. After phase separation (b and c), the interior solution consists of two liquid droplets consisting of PEG-rich and dextran-rich phases, respectively. Since the latter phase has the larger mass density, the dextran-rich droplet is located beneath the PEG-rich one. Further deflation of the vesicle causes the dextran-rich droplet to bud out as shown in (d) and (e). The dense phase at the lower part of the vesicle is the dextran-rich phase. The light part is the PEG-rich phase. The numbers on the snapshots indicate the osmolarity ratio between the external medium and the initial internal polymer solution. In the sketch in (f), the three effective contact angles as observed with optical microscopy are indicated, as well as the two membrane tensions and the interfacial tension Σ_{pd} . The contact line is indicated by the circled dot \odot . The intrinsic contact angle θ_{in} , which characterizes the wetting properties of the membrane by the PEG-rich phase at the nanometre scale, is sketched in (g).

can be reversed if the phase separation occurs in the vesicle exterior.¹⁴

In mechanical equilibrium, the two membrane tensions $\hat{\Sigma}_{pe}$ and $\hat{\Sigma}_{de}$ must be balanced along the contact line (where the external medium, the PEG-rich phase and the dextran-rich phase are in close proximity) by the interfacial tension Σ_{pd} between the two liquid phases, see Fig. 3f. The interfacial tension Σ_{pd} pulls on the membrane towards the vesicle interior. When Σ_{pd} is small, the membrane tensions can easily balance this pulling force in the normal direction and the contact angle θ_e remains close to 180 degrees. The excess area arising from deflation can be stored in the form of lipid aggregates or nanotubes,¹³ as we will discuss further below, and the vesicle can remain quasi-spherical. As the interfacial tension Σ_{pd} increases and the vesicle is deflated further (creating more excess area), the membrane tension can no longer sustain the quasi-spherical vesicle shape. Because the membrane is very flexible it bends along the contact line and budding of the dextran-rich phase occurs as the vesicle is further deflated. The budding event significantly reduces the interfacial energy by decreasing the contact area between the liquid phases. A

detailed theoretical analysis of the budding transition accounting for the competition between bending and surface forces was recently reported for the case where one of the phases (the budding droplet) is much smaller than the other one.²⁰

Intrinsic contact angle

When viewed with optical resolution, the membrane of budded vesicles, as in Fig. 3d and e, exhibits a kink along the contact line, see the sketch in Fig. 3f. From the microscopy images one can measure the effective contact angles θ_d , θ_p and θ_e , see Fig. 3f, and relate them to the tensions $\hat{\Sigma}_{de}$, $\hat{\Sigma}_{pe}$ and Σ_{pd} . However, if the membrane shape had a kink that persisted to smaller length scales, its bending energy would become infinite. Therefore, when viewed with suboptical resolution, the membrane should be smoothly curved, which implies the existence of an intrinsic contact angle θ_{in} as sketched in Fig. 3g. Indeed, minimization of the membrane bending energy together with the force balance along the three phase contact line shows that the intrinsic angle is related to the effective contact angles via $\cos \theta_{in} = (\sin \theta_p - \sin \theta_d) / \sin \theta_e$.¹² Thus,

θ_{in} can be estimated from experimentally measurable parameters, namely the effective contact angles as obtained from microscopy images. Whereas the effective contact angles and the tensions $\hat{\Sigma}_{de}$ and $\hat{\Sigma}_{pe}$ depend on the vesicle geometry, the intrinsic contact angle is a material parameter, which arises from the molecular interactions between the phases and the membrane. Since the intrinsic contact angle is not measurable directly in budded vesicles, it represents a “hidden variable” within the system. In quasi-spherical vesicles, for which the effective contact angle θ_e is close to 180 degrees, as those discussed in the section Wetting transition, the intrinsic contact angle θ_{in} can be estimated by the effective contact angle θ_p .

Formation of membrane nanotubes in vesicles containing aqueous two-phase systems

In this section, we will discuss a particular morphological transition of membranes in contact with two-phase systems. Upon vesicle deflation, excess area is created. Depending on the membrane properties, such as membrane tension and

spontaneous curvature, the area created during deflation may lead to vesicle budding, as shown in the section Wetting-induced budding, and/or may be involved in creating membrane nanotubes.¹³ In this section, we will discuss this second case.

Studies on membrane tubes are of particular interest because of their relevance to cellular structures. Eukaryotic cells often contain tubular membrane structures, also known as tethers or membrane nanotubes, with dimensions ranging from a few microns in diameter (myelin structures) to a few tens of nanometres. They are constantly formed in the Golgi apparatus and in mitochondria,^{21,22} as well as in the smooth endoplasmic reticulum (ER), a tubular membranous structure²³ with tube diameters of 50–150 nm. There, newly synthesized lipids have to be stored before being

transferred to their target destinations. Folding excess membrane into tubes provides a very efficient way to store this membrane, because the tubes are characterized by a relatively large area-to-volume ratio.

In a number of previous studies, tubes have been pulled from cells and model membranes by applying an external force *via* fluid drag,^{24–27} gravity,²⁸ micropipette systems,^{29,30} or optical^{31,32} and magnetic tweezers.^{33,34} The forces needed for pulling membrane tubes from Golgi or ER membranes are on the order of 10 pN.³⁵ In all of these studies, tube formation required the local application of an external force. In contrast, tube formation in vesicles exhibiting aqueous phase separation does not involve such an external force but may also play a role in organizing the membrane of cellular organelles into tubular structures.

Tubes formed in vesicles enclosing two phase-separated drops have a diameter below optical resolution and become visible only when fluorescently labeled. The tubes form during the phase separation process and are stable after this process has been completed. Tube formation can be directly observed, see Fig. 4. Before deflation, no fluorescence is detected in the vesicle interior, Fig. 4a. When the osmolarity of the external medium is increased, phase separation is initiated and small droplets of the dextran-rich phase are observed inside the vesicle, see Fig. 4b. After phase separation is completed, a collection of membrane tubes always in contact with the PEG-rich phase is observed, Fig. 4c and d. At higher osmolarity ratios between the external medium and the initial internal polymer solution, the excess membrane adsorbs at the two-phase interface forming a layer or meshwork of tubes, Fig. 4e and f. As the excess area of the membrane increases and the contact area between the PEG-rich and dextran-rich phases decreases, the interface becomes overcrowded and the tubes start to protrude partially into the PEG-rich phase, see Fig. 4g and h. Confocal scans of the horizontal plane slightly above the interface can show circular tube cross-sections with a diameter of about 1 μm for certain osmolarity conditions, see Fig. 4i.

A theoretical analysis of the deflated vesicles reveals that these membrane tubes are stabilized by spontaneous curvature.¹³ Using the large separation of length scales between the tube diameter and the overall size of the vesicles, the spontaneous curvature can be calculated and is found to be negative and on the order of $-1/(240 \text{ nm})$ for a certain range of polymer concentrations. The theoretical analysis also shows that the tube formation can be understood from the competition of two opposing constraints acting on the pe membrane segment located between the PEG-rich phase and the external solution. On the one hand, the membrane is forced to enclose a certain volume of PEG-rich phase. This volume constraint necessarily implies that a large segment of the pe membrane must curve towards the PEG-rich phase. However, because of its negative spontaneous curvature, the pe membrane would really prefer to curve in the opposite way, *i.e.*, towards the

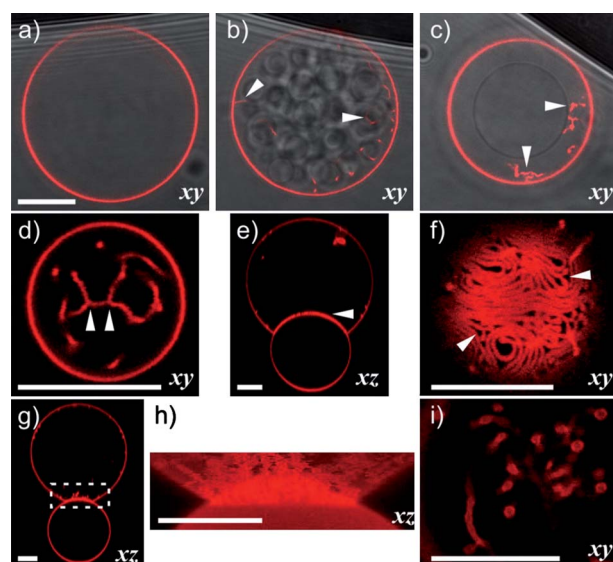


Fig. 4 Tube formation in vesicles with internal phase separation. The polymer molecular weights and the membrane composition are the same as in Fig. 2. (a–c) Overlay of top-view confocal sections and bright field images of a vesicle (a) before deflation, (b) during phase separation and (c) after 2.6 hours of equilibration. The arrowheads in (b) and (c) indicate fluorescence from tubes in the focal plane. The droplets visible in (b) contain the newly formed dextran-rich phase. In (c), the inner dark circle represents the contour of the dextran-rich phase, which is in focus. The out-of-focus outer dark circle is the contour of the PEG-rich phase above the dextran-rich phase. The fluorescent signal shows the membrane crossing the focal plane. (d) Confocal xy -section of another vesicle showing possible three-way tube junctions indicated by arrows, as in (f). For (c) and (d), the osmolarity ratio between the external medium and the initial internal polymer solution is 1.24. (e) Vertical xz -section showing adsorption of tubes onto the two-phase interface. (f) Horizontal xy -section at the z -position of the arrowhead in (e) showing tubes at the two-phase interface. (g) Vertical xz -section of a vesicle with an overcrowded two-phase interface; the tubes protrude into the upper PEG-rich phase. (h) 3D projection from a stack of xy -sections at the two-phase interface delimited by the rectangle in (g). (i) Confocal xy -section of the tubes slightly above the two-phase interface. For (e)–(i), the osmolarity ratio between the external medium and the initial internal polymer solution is 1.5. The scale bars correspond to 15 μm . Reproduced from ref. 13.

external phase. The latter curvature can be achieved *via* membrane nanotubes that form inside the vesicle and, thus, enwrap only small volumes of external phase. As a consequence, the pe membrane forms many such nanotubes and one large segment around the PEG-rich droplet, the latter segment adopting a spherical cap shape in order to minimize its area.

Tubes are relevant for membrane storage in cells. With the vesicle system exhibiting internal phase separation we observe that as much as 15% of a vesicle membrane area can be stored in tubes.¹³ Even though the structure, purpose and functions of tubular membranous networks such as the trans-Golgi network and the smooth ER have been studied for a long time, the physical mechanism and driving forces involved in their formation and restructuring remain elusive. Actin polymerization^{36,37} and molecular motors^{38–40} may play a role in pulling membrane tubes. However, cytoskeletal filaments are not in abundance in the smooth ER. Our findings on vesicles enclosing phase separated solutions suggest that membrane restructuring in the smooth ER may be governed by another mechanism, namely local phase separation of the crowded environment in the cell interior and spontaneous curvature stabilization.

The nanotubes formed in the ATPS can also be retracted back into the mother vesicle by increasing the membrane tension *via* micropipette aspiration of the vesicle.¹³ A tension threshold is observed, above which the tubes start to retract to the vesicle body. The existence of this tension threshold shows that cells could switch retraction on and off when needed. Tubes which form and recede easily might be relevant to surface area regulation in cells. Many cells, including growing neurons and dividing cells, undergo rapid volume and surface area changes. This requires a quick exchange of membrane between the surface and the internal sources. Tubes could act as internal area reservoirs, from which the membrane can be easily recruited back. This area recruitment involves the control of the membrane tension, which can be varied by the osmotic conditions, or dynamic morphological changes such as the formation of a metastable raspberry-like surface.¹³

Conclusions and perspectives

As we have demonstrated above, studies on ATPS-loaded vesicles may lead to a deeper understanding of membrane behavior and membrane processes *in vivo*, such as membrane budding and fission, membrane adhesion and fusion, or transport of membranes and vesicles.

Of particular interest is to understand the mechanism of how membrane curvature is generated by aqueous phases. Our studies performed on the micron-size level reveal the overall morphological change of the vesicle. On the scale of a few nanometres, we were able to deduce the existence of an intrinsic contact angle and to estimate its value. What we are not yet able to resolve are possible conformational changes of the macromolecules (such as proteins in cells or polymers in the model system considered in more detail here) and their interaction with the lipid bilayer or membrane-anchored molecules. A challenging task is to correlate, in a quantitative manner, the membrane interactions and behavior at the nanometre scale with the morphological response at the micrometre scale. In the previous section, we illustrated this relation *via* one example, namely, membrane curvature generated by aqueous polymer phases. Understanding the molecular origin of this curvature generation and ways to control it would be helpful for understanding related cellular mechanisms, such as *endo*- and *exo*-cytosis and vesicle trafficking. Some progress in this direction is already available for lipid and polymer membranes with varied bilayer composition^{41–44} or for membranes in the presence of curvature modulating or curvature sensing proteins,^{45–49} but membranes in contact with ATPSs have not been explored so far.

In fact, as we demonstrated here, ATPS-loaded vesicles provide a unique opportunity to determine the spontaneous curvature of the membranes, as induced by their interactions with nanostructures and macromolecules. So far, no reliable methods for direct measurement of the membrane spontaneous curvature are available. Probably the best approach is based on an analysis of membrane undulations,^{50,51} but it requires the generation of reference data *via* extensive Monte Carlo simulations.⁵² Other

methods measure only the spontaneous curvature of lipid molecules and can be applied solely to lipids forming an inverted hexagonal phase^{53,54} or to membranes with fluorescent analogues.⁵⁵ In contrast, vesicles with ATPS provide a new and direct approach to systematically evaluate the membrane spontaneous curvature from optically measured contact angles and the associated membrane tensions.

Studies on ATPS-loaded vesicles are important even though aqueous phase separation has not been directly observed in the majority of cell types yet. Presumably, this is so either because of the large number of molecule types present, or because of the limiting resolution of the techniques employed. Many protein bodies and puncta in cells⁵⁶ may, in fact, be liquid droplets, as recently demonstrated for P-granules in the germ cells of *C. elegans*.⁵⁷ Phase separation within the eye lens cytoplasm during aging leads to the loss of vision experienced with cataracts.^{58,59} These are just a few examples of aqueous phase separation in cells, which is crucial for microcompartmentation and protein relocalization. The physical chemistry of aqueous solutions of polymers and biomacromolecules offers a convenient pathway for addressing these issues as well as membrane-related processes in cells.

Acknowledgements

We thank Yanhong Li, Halim Kusumaatmaja, and Yonggang Liu for enjoyable collaborations.

References

- 1 T. Schwarz-Romond, C. Merrifield, B. J. Nichols and M. Bienz, *J. Cell Sci.*, 2005, **118**, 5269–5277.
- 2 R. P. Sear, *Soft Matter*, 2007, **3**, 680–684.
- 3 P. Å. Albertsson, *Partition of Cell Particles and Macromolecules: Separation and Purification of Biomolecules, Cell Organelles, Membranes, and Cells in Aqueous Polymer Two-Phase Systems and Their Use in Biochemical Analysis and Biotechnology*, Wiley, New York, 1986, 3rd edn.
- 4 J. van der Gucht, E. Spruijt, M. Lemmers and M. A. C. Stuart, *J. Colloid Interface Sci.*, 2011, **361**, 407–422.
- 5 M. R. Helfrich, L. K. Mangeney-Slavin, M. S. Long, Y. Djoko and C. D. Keating, *J. Am. Chem. Soc.*, 2002, **124**, 13374–13375.
- 6 M. S. Long, C. D. Jones, M. R. Helfrich, L. K. Mangeney-Slavin and C. D. Keating,

- Proc. Natl. Acad. Sci. U. S. A.*, 2005, **102**, 5920–5925.
- 7 L. M. Dominak, E. L. Gundermann and C. D. Keating, *Langmuir*, 2010, **26**, 5697–5705.
- 8 M. S. Long, A. S. Cans and C. D. Keating, *J. Am. Chem. Soc.*, 2008, **130**, 756–762.
- 9 Y. Li, R. Lipowsky and R. Dimova, *J. Am. Chem. Soc.*, 2008, **130**, 12252–12253.
- 10 R. Dimova, S. Aranda, N. Bezlyepkina, V. Nikolov, K. A. Riske and R. Lipowsky, *J. Phys.: Condens. Matter*, 2006, **18**, S1151–S1176.
- 11 A. S. Cans, M. Andes-Koback and C. D. Keating, *J. Am. Chem. Soc.*, 2008, **130**, 7400–7406.
- 12 H. Kusumaatmaja, Y. Li, R. Dimova and R. Lipowsky, *Phys. Rev. Lett.*, 2009, **103**, 238103.
- 13 Y. Li, R. Lipowsky and R. Dimova, *Proc. Natl. Acad. Sci. U. S. A.*, 2011, **108**, 4731–4736.
- 14 Y. Li, H. Kusumaatmaja, R. Lipowsky and R. Dimova, *J. Phys. Chem. B*, 2012, **116**, 1819–1823.
- 15 A. Kaul, in *Aqueous Two-Phase Systems: Methods and Protocols*, 2000, vol. 11, pp. 11–21.
- 16 Y. Liu, R. Lipowsky and R. Dimova, *Langmuir*, 2012, **28**, 3831–3839.
- 17 J. Ryden and P. Å. Albertsson, *J. Colloid Interface Sci.*, 1971, **37**, 219–222.
- 18 E. Cocucci, G. Racchetti and J. Meldolesi, *Trends Cell Biol.*, 2009, **19**, 43–51.
- 19 M. Andes-Koback and C. D. Keating, *J. Am. Chem. Soc.*, 2011, **133**, 9545–9555.
- 20 H. Kusumaatmaja and R. Lipowsky, *Soft Matter*, 2011, **7**, 6914–6919.
- 21 M. A. De Matteis and A. Luini, *Nat. Rev. Mol. Cell Biol.*, 2008, **9**, 273–284.
- 22 G. Benard and R. Rossignol, *Antioxid. Redox Signaling*, 2008, **10**, 1313–1342.
- 23 C. Lee and L. B. Chen, *Cell*, 1988, **54**, 37–46.
- 24 R. M. Hochmuth, N. Mohandas and P. L. Blackshear, *Biophys. J.*, 1973, **13**, 747–762.
- 25 R. E. Waugh, *Biophys. J.*, 1982, **38**, 29–37.
- 26 D. W. Schmidtke and S. L. Diamond, *J. Cell Biol.*, 2000, **149**, 719–729.
- 27 S. M. Dopheide, M. J. Maxwell and S. P. Jackson, *Blood*, 2002, **99**, 159–167.
- 28 L. Bo and R. E. Waugh, *Biophys. J.*, 1989, **55**, 509–517.
- 29 R. M. Hochmuth, H. C. Wiles, E. A. Evans and J. T. McCown, *Biophys. J.*, 1982, **39**, 83–89.
- 30 D. Cuvelier, I. Derenyi, P. Bassereau and P. Nassoy, *Biophys. J.*, 2005, **88**, 2714–2726.
- 31 R. M. Hochmuth, J. Y. Shao, J. W. Dai and M. P. Sheetz, *Biophys. J.*, 1996, **70**, 358–369.
- 32 R. Dimova, U. Seifert, B. Pouligny, S. Förster and H.-G. Döbereiner, *Eur. Phys. J. B*, 2002, **7**, 241–250.
- 33 V. Heinrich and R. E. Waugh, *Ann. Biomed. Eng.*, 1996, **24**, 595–605.
- 34 B. G. Hosu, M. Sun, F. Marga, M. Grandbois and G. Forgacs, *Phys. Biol.*, 2007, **4**, 67–78.
- 35 A. Upadhyaya and M. P. Sheetz, *Biophys. J.*, 2004, **86**, 2923–2928.
- 36 D. Pantaloni, C. Le Clainche and M. F. Carlier, *Science*, 2001, **292**, 2012.
- 37 A. Rustom, R. Saffrich, I. Markovic, P. Walther and H. H. Gerdes, *Science*, 2004, **303**, 1007–1010.
- 38 A. Roux, G. Cappello, J. Cartaud, J. Prost, B. Goud and P. Bassereau, *Proc. Natl. Acad. Sci. U. S. A.*, 2002, **99**, 5394–5399.
- 39 G. Koster, M. VanDuijn, B. Hofst and M. Dogterom, *Proc. Natl. Acad. Sci. U. S. A.*, 2003, **100**, 15583–15588.
- 40 C. Leduc, O. Campas, K. B. Zeldovich, A. Roux, P. Jolimaitre, L. Bourel-Bonnet, B. Goud, J. F. Joanny, P. Bassereau and J. Prost, *Proc. Natl. Acad. Sci. U. S. A.*, 2004, **101**, 17096–17101.
- 41 A. Tian and T. Baumgart, *Biophys. J.*, 2009, **96**, 2676–2688.
- 42 M. Heinrich, A. Tian, C. Esposito and T. Baumgart, *Proc. Natl. Acad. Sci. U. S. A.*, 2010, **107**, 7208–7213.
- 43 B. Sorre, A. Callan-Jones, J. B. Manneville, P. Nassoy, J. F. Joanny, J. Prost, B. Goud and P. Bassereau, *Proc. Natl. Acad. Sci. U. S. A.*, 2009, **106**, 5622–5626.
- 44 E. Mabrouk, D. Cuvelier, F. Brochard-Wyart, P. Nassoy and M. H. Li, *Proc. Natl. Acad. Sci. U. S. A.*, 2009, **106**, 7294–7298.
- 45 B. J. Peter, H. M. Kent, I. G. Mills, Y. Vallis, P. J. G. Butler, P. R. Evans and H. T. McMahon, *Science*, 2004, **303**, 495–499.
- 46 A. Roux, G. Koster, M. Lenz, B. Sorre, J. B. Manneville, P. Nassoy and P. Bassereau, *Proc. Natl. Acad. Sci. U. S. A.*, 2010, **107**, 4141–4146.
- 47 B. R. Capraro, Y. Yoon, W. Cho and T. Baumgart, *J. Am. Chem. Soc.*, 2010, **132**, 1200–1201.
- 48 T. R. Graham and M. M. Kozlov, *Curr. Opin. Cell Biol.*, 2010, **22**, 430–436.
- 49 T. Baumgart, B. R. Capraro, C. Zhu and S. L. Das, *Annu. Rev. Phys. Chem.*, 2011, **62**, 483–506.
- 50 H. G. Döbereiner, E. Evans, M. Kraus, U. Seifert and M. Wortis, *Phys. Rev. E: Stat. Phys., Plasmas, Fluids, Relat. Interdiscip. Top.*, 1997, **55**, 4458–4474.
- 51 V. Nikolov, R. Lipowsky and R. Dimova, *Biophys. J.*, 2007, **92**, 4356–4368.
- 52 H. G. Döbereiner, G. Gompper, C. K. Haluska, D. M. Kroll, P. G. Petrov and K. A. Riske, *Phys. Rev. Lett.*, 2003, **91**, 4.
- 53 R. P. Rand, N. L. Fuller, S. M. Gruner and V. A. Parsegian, *Biochemistry*, 1990, **29**, 76–87.
- 54 N. Fuller and R. P. Rand, *Biophys. J.*, 2001, **81**, 243–254.
- 55 M. M. Kamal, D. Mills, M. Grzybek and J. Howard, *Proc. Natl. Acad. Sci. U. S. A.*, 2009, **106**, 22245–22250.
- 56 M. J. Smalley, N. Signoret, D. Robertson, A. Tilley, A. Hann, K. Ewan, Y. N. Ding, H. Paterson and T. C. Dale, *J. Cell Sci.*, 2005, **118**, 5279–5289.
- 57 C. P. Brangwynne, C. R. Eckmann, D. S. Courson, A. Rybarska, C. Hoeghe, J. Gharakhani, F. Julicher and A. A. Hyman, *Science*, 2009, **324**, 1729–1732.
- 58 C. W. Liu, N. Asherie, A. Lomakin, J. Pande, O. Ogun and G. B. Benedek, *Proc. Natl. Acad. Sci. U. S. A.*, 1996, **93**, 377–382.
- 59 J. I. Clark and J. M. Clark, *International Review of Cytology – A Survey of Cell Biology*, 2000, vol. 192, pp. 171–187.

Addition and correction

[View Online](#)

Note from RSC Publishing

This article was originally published with incorrect page numbers. This is the corrected, final version.

The Royal Society of Chemistry apologises for these errors and any consequent inconvenience to authors and readers.
